Determination of major elements in Antarctic snow by inductively coupled plasma optical emission spectrometry using a total-consumption sample introduction system

(Article begins on next page)

18 May 2024

Determination of major elements in Antarctic snow by inductively coupled plasma optical emission spectrometry using a total-consumption sample introduction system

Stefano Bertinetti,[a] Francisco Ardini,[a] Laura Caiazzo[b,c] and Marco Grotti[a,*]

[a] *Department of Chemistry and Industrial Chemistry, University of Genoa, Via Dodecaneso 31, 16146, Genoa, Italy*

[b] *Department of Chemistry Ugo Schiff, University of Florence, Via della Lastruccia 3, 50019, Sesto Fiorentino, Italy*

[c] *INFN-Florence, Via Sansone 1, 50019, Sesto Fiorentino, Italy*

Abstract

A new procedure for the determination of Al, Ba, Ca, Fe, K, Mg, Na and Sr in snow samples by inductively coupled plasma optical emission spectrometry (ICP-OES) has been developed. The analytes were 100-fold preconcentrated by sample volume reduction and quantified by ICP-OES using the heated torch-integrated sample introduction system (hTISIS). After multivariate optimization of the hTISIS/ICP-OES operating parameters for maximum sensitivity and plasma robustness, fit-for-purpose performances were achieved, requiring only 20 mL of sample (as water equivalent). The analytical recovery was quantitative (except for Ba at low concentration, $\approx 80\%$) and the precision of the procedure was better than 5%. The limits of detection (Al: 0.10 ng g^{-1}; Ba: 0.013 ng g^{-1}; Ca: 0.52 ng g^{-1}; Fe: 0.13 ng g^{-1}; K: 0.38 ng g^{-1}; Mg: 0.04 ng g^{-1}; Na: 0.39 ng g^{-1}; Sr: 0.003 ng g^{-1}) were suitable for the analysis of Antarctic snow, with some limitation for Ba. The accuracy and uncertainty of the method were assessed by the analysis of the certified reference water NIST SRM 1640a. The application of the analytical method to sixty snow samples collected at Dome C, on the East Antarctic Plateau, provided self-consistent results, in good agreement with literature data.

* Corresponding author. e-mail: grotti@chimica.unige.it

1. Introduction

Antarctic snow and ice are unique archives for past environmental conditions, providing direct and highly resolved records of atmospheric parameters and their variability through time.[1,2] However, a more accurate interpretation of these glaciochemical records still requires a better understanding of the factors that control the snow chemistry, including the atmospheric transport of aerosols, precipitation processes and post-depositional effects.[3,4] In this context, the chemical analysis of snow samples plays a central role, due to the relevant information that can be obtained by using various elemental proxies, such as those derived from the quantification of the alkaline and alkaline-earth elements, aluminum and iron. For example, sodium is a reliable sea-spray marker,[5,6] whereas aluminum and barium are useful indicators of the continental crustal contribution.[7,8] Iron determination in Antarctic snow is also of great importance, both as a marker of the mineral dust and to elucidate the impact of iron fertilization on the carbon dioxide sequestration in the Southern Ocean.[9,10,11]

These elements are present in the Antarctic snow and ice at very low concentration levels, typically at or below ng g^{-1}, thus requiring analytical methods with high sensitivity and precision. Besides, the applied analytical protocols have to assure ultra-clean conditions, from the sampling to the instrumental analysis, with a strict control and evaluation of any possible source of contamination. Finally, in order to obtain an adequate vertical resolution for the study of the temporal variation of the chemical parameters, the amount of sample for the analysis should be as low as possible.

The determination of major ions in Antarctic snow is usually carried out by ion chromatography.[12,13,14] However, this technique is basically limited to Na^+, K^+, Ca^{2+} and Mg^{2+} and, whenever the study requires the determination of other major elements (*e.g.* Al, Ba, Fe), additional instrumental techniques have to be applied, such as inductively coupled plasma optical emission spectrometry (ICP-OES)[6,15,16,17] and inductively coupled plasma mass spectrometry (ICP-MS).[7,18,19]

In this work, we developed a new method based on ICP-OES to carry out the simultaneous determination of Al, Ba, Ca, Fe, K, Mg, Na and Sr in Antarctic snow samples, requiring just 20 mL (as water-equivalent, corresponding to ≈50 mL of snow) of each sample. The method combines a simple and clean pre-concentration procedure with the use of a total-consumption sample introduction system which allows the ICP-OES analysis to be completed while consuming less than 200 µL of pre-concentrates and the attaining of high sensitivity and

2

precision. After the multivariate optimization of the operating conditions, the method was fully characterised in terms of precision and accuracy, sensitivity, analytical recovery and limits of detection, and finally applied to sixty snow samples from the Antarctic plateau. It is demonstrated that ICP-OES performances can be improved to a level that allows to face even this demanding application, providing a new analytical tool for the environmental studies in the polar regions.

2. Experimental

2.1. Instrumentation

The Thermo-Fisher Scientific (Waltham, MA, USA) iCAP 6000 ICP-OES Duo instrument was used, selecting the axial plasma view for any wavelength to achieve the best sensitivity and detection limits. The instrumental and operating conditions are summarised in Table 1.

The sample introduction system was the so-called heated torch-integrated sample introduction system (hTISIS),[20,21,22] consisting of a single-pass spray chamber, with a lateral port to introduce a sheathing gas stream in a location close to the aerosol production point. A Teflon adapter was used to fit a PFA-ST micronebulizer by Elemental Scientific (Omaha, NE, USA) to the chamber base, and the cavity was directly jointed with the quartz injector of the plasma torch. The chamber was electrically heated at 150 °C by means of a wounded heating tape connected to a DC power supply. For comparison purposes, a Glass Expansion (Melbourne, Australia) Cinnabar spray chamber with a 20-mL inner volume was also used.

2.2. Reagents and materials

Ultrapure water was supplied by the four-column ion-exchange system Milli-Q fed by the reverse osmosis system Elix 3, both from Millipore (Burlington, MA, USA). Ultrapure-grade Normatom® 67% nitric acid from VWR International (Radnor, PA, USA) and TraceSELECT® Ultra 49% hydrofluoric acid from Honeywell Fluka (Charlotte, NC, USA) were used for sample preparation. 1000 mg L^{-1} single-element standard solutions were obtained from Fluka and Merck (Darmstadt, Germania), and properly diluted to the final concentration (see Table S1 (Appendix)) with Milli-Q water.

2.3. Samples

A continuous series of snow samples was obtained in 2017 at Dome C, East Antarctic Plateau, from the wall of a 4-m-deep pit, corresponding to the period 1971-2017. Samples were collected in 50-mL pre-cleaned polypropylene tubes and stored at -20 °C until analysis. Details on the sampling site, the collection procedure and the sample dating have been previously reported.[23]

For method validation, the standard reference material SRM 1640a from the National Institute of Standards & Technology (NIST, Gaithersburg, MD, USA) was used.

2.4. Pre-concentration procedure

The pre-concentration of snow samples was carried according to a procedure previously developed for the ICP-MS determination of trace elements[24] and lead isotopic ratios.[25] Briefly, the samples were allowed to melt in their closed tubes and weighed to determine the exact mass (≈20 g). Subsequently, the samples were acidified at 0.5% (v/w) with HNO_3 and HF, left closed for 24 h, and refrozen. Then, the samples were freeze-dried and redissolved in 200 µL of 0.05% HNO_3, providing a pre-concentration factor of ≈100 (accurately computed for each sample).

Procedural blanks and standard solutions for the recovery tests were concomitantly prepared exactly as the snow samples, using 20 mL of Milli-Q water.

2.5. Multivariate experiments and data processing

The combined effect of the operating conditions on the analytical signals was investigated by an experimental design-based approach,[26] applying a faced central composite design (see Table S2 (Appendix)). In each condition, the emission intensities at 32 wavelengths (Table 1) were measured for the standard solution 3 (see Table S1 (Appendix)). To minimize the influence of systematic trends (*e.g.* instrumental drift), the experiments were performed randomly. Runs 25-28 (replicates at the center point) were performed regularly throughout the sequence of analysis to give the estimate of the experimental variance, necessary to evaluate the significance of the models' coefficients. After a judicious selection of the detector sub-arrays for appropriate peak and background measurements, raw data were exported and processed using the open-source software *R*,[27] with the additional package *CAT*.[28] Principal Component Analysis (PCA) was performed using the same software tools, after autoscaling of data.

Plasma robustness was evaluated by the Mg 280.270 nm (ionic line) to Mg 285.213 nm (atomic line) intensity ratio (MgR).[29] Values were corrected for differences in response due to the use of an echelle grating, by applying a factor of 1.4 (empirically determined by ratioing the background emission at the wavelengths corresponding to the atomic and ionic lines).

3. Results and discussion

3.1. Optimization of the operating conditions

Due to the low analytical concentration expected in the Antarctic snow samples, the first step of the method development was the optimization of the ICP-OES operating conditions to achieve the best sensitivity and sufficient plasma robustness. The combined effect of RF power (P), nebulizer pressure (NP), sheathing gas flow rate (SG) and sample uptake rate (UR) on the analytical signals was studied by applying a central composite design, as described above. The obtained responses (emission intensities at the wavelengths listed in Table 1), were firstly analyzed by applying a PCA to the data matrix formed by the 28 experiments (see Table S2 (Appendix)) and the 32 responses, finding that the 94% of the total variance of data is explained by the first PC (PC1). Therefore, the score of the experiments on this PC was considered as a new response, being a linear combination of the 32 original ones. This transformation significantly simplified the following regression analysis, since only two models had to be studied: PC1 (to collectively consider all the analytical signals) and MgR (for plasma robustness).

The coefficients of the models and their significance are reported in Table S3 (Appendix) and S4 (Appendix), and representative response surfaces are shown in Figure 1. It can be observed that an increase in the RF power led to an improvement of sensitivity (Figure 1a,b), likely due to the enhanced plasma excitation conditions, as highlighted by a concomitant increase in MgR (Figure 1d,e). The effect on sensitivity was higher at high sample uptake rates (Figure 1b,e), when the solvent load increased, thus requiring more energy from the plasma source. The sensitivity also increased by decreasing the nebulizer pressure and sheathing gas flow rate, with a strong interaction between these parameters (Figure 1c). This trend can be explained considering that the decrease in the nebulizer gas flow rate reduces the droplet velocity inside the chamber and, hence, the impacts against the cavity walls. In addition, by reducing the nebulizer and sheathing gas flow rates, the sample residence time within the plasma source increases.

Accordingly, MgR values also increased by decreasing the gas flow rates (Figure 1f), indicating more robust plasma conditions.

By analysing the response surfaces, the following optimal conditions were selected: maximum RF power (1350 W), lowest values of nebulizer pressure (0.15 MPa) and sheathing gas flow rate (0.1 L min^{-1}) and a sample uptake rate of 50 µL min^{-1}. In fact, the increase of the uptake rate led to an increase of sensitivity (Fig. 1b) but to a decrease of MgR values (Fig. 1e). Consequently, a compromise value had to be chosen in order to match high emission intensities and sufficient plasma robustness (MgR=9.5±0.4). Finally, the models were validated by replicated analysis of standard 3 under the optimal conditions. The prediction errors were -1% and 6% for PC1 and MgR, respectively, and the models were hence considered fit-to-purpose.

3.2. Instrumental performances

The performances of ICP-OES measurements under the optimal conditions are gathered in Table 2. The concentration ranges were selected according to the expected concentration in the Antarctic snow samples as reported by previous investigations (*e.g.* Refs 8,17), considering a pre-concentration factor of 100 due to the sample preparation procedure. Within each concentration range, the signal intensity varied linearly, at any wavelengths. The sensitivity, computed as the slope of the calibration curve, resulted about 2 times better than that obtained using a conventional sample introduction system, working at the same sample uptake rate. The instrumental precision was better than 5% (usually better than 2%), except for the Sr 346.446 nm emission line, which was not used for the analysis of the samples because of its low sensitivity. Similarly, it was decided to remove few other emission lines (highlighted in italic in Table 1). The signal variation during a 3-h analytical session ranged from 2.1 to 5.3%.

3.3. Pre-concentration procedure: analytical recovery, precision and limits of detection

Despite the optimization of the instrumental parameters and the use of a high-efficiency sample introduction system, the achieved sensitivity was inadequate for the direct analysis of Antarctic snow samples, thus requiring the application of a sample pre-concentration step. In previous studies, a simple and clean procedure has been developed and successfully applied for the determination of trace elements[17,24] and lead isotopic ratios[23,25,30] in Antarctic snow samples. The procedure is based on solvent removal by freeze-drying and it allows a pre-concentration factor of ≈100 to be achieved by reducing the sample volume from ≈20.0 to 0.2 mL. The first

6

volume corresponds to the water obtained by melting the snow collected into 50-mL polypropylene tubes, which enables the sampling from snow pits with high vertical resolution (≈3 cm). The final volume of 200 µL is the minimum amount necessary to reconstitute the sample after the freeze-drying step and to perform the multi-element ICP-OES analysis using the low-sample consumption hTISIS system.

In order to validate the procedure for the analytes considered in this work, a number of procedural blanks and standard solutions were prepared exactly as the snow samples and analyzed by ICP-OES. The results are reported in Table 3. A quantitative recovery can be observed for all the analytes (except for Ba at low concentration, ≈80%), with a good agreement among the results at the various wavelengths. The analytical precision was always better than 5%. Finally, the detection limits computed by the analysis of ten procedural blanks according to the 3σ-criterion proved to be adequate for the analysis of Antarctic snow samples, with some limitation for barium, as discussed below.

3.4. Accuracy and uncertainty estimation

The accuracy of the analytical method was finally verified by using the certified natural water SRM 1640a, supplied by NIST. In order to match the certified analytical concentrations with the real ones, the standard was 20-fold diluted for the determination of Al, Fe, K, Mg, Na and 2000-fold diluted for the determination of Ba, Ca and Sr. Then, 20-mg aliquots were freeze-dried, re-dissolved in 200 µL of 0.05% nitric acid solution and analyzed by ICP-OES.

The results are reported in Table 4. The uncertainty associated to each value is the expanded uncertainty about the mean calculated following the GUM guideline.[31] In particular, the uncertainty sources in the final concentration values are related to the instrumental precision of the analysis of both sample and blank solutions, the uncertainties of the regression parameters, and errors in the sample mass (determined by differential weighting before and after the freeze-drying procedure) and in the final volume of nitric acid for sample redissolution. Instrumental precision was determined by the replicates of each measurement, whereas the uncertainties in mass and volume values were empirically estimated by replicating each measurement 30 times and computing the standard deviation of the obtained values. The errors in the slope and intercept of the calibration curve were determined according to the ordinary least squares statistics. Finally, the single uncertainty components were combined according to the random error propagation

laws and the combined uncertainty was finally multiplied by the coverage factor of 2 to give the expanded uncertainty.

It can be seen that the method provided accurate results, with differences between found and certified values lower than 8.5% and precision better than 2.4% (relative combined uncertainty, n=5), in agreement with the recovery tests.

3.5. Application to Antarctic snow samples

The developed method was finally applied to sixty snow pit samples collected at Dome C, on the East Antarctic Plateau,[23] and the results are collectively displayed in Figure 2. While a thorough discussion of these data in the context of the environmental studies is out of the scope of this paper, the results attained were briefly analyzed to assess the applicability of the proposed method to the analysis of Antarctic snow samples.

Firstly, it was observed that the limits of detection were adequate for the analytical task, except for barium that was detected only in 25% of the samples. However, higher barium concentration can be found in Antarctic snow (*e.g.* 0.062-22 ng g^{-1} in snow near South Pole[19]), and the proposed method could also be suitable for this trace element in specific investigations. Furthermore, the analytical data here obtained are in good agreement with values reported in many previous studies in Antarctica, as summarized in Table S5 (Appendix). Finally, a simple correlation analysis revealed a significant correlation ($p < 0.01$) between Fe and Al, as well as among the alkaline and alkaline-earth elements, as expected by the typical prevalent sources of these elements (crustal and marine, respectively).

4. Conclusions

The accurate determination of Al, Ca, Fe, K, Mg, Na and Sr in Antarctic snow samples can be achieved by combining a simple and clean pre-concentration procedure with ICP-OES equipped with hTISIS. The developed method has fit-for-purpose performances and it requires only 20 mL of sample (as water equivalent), permitting a good sampling resolution. The method could also be suitable for Ba determination, provided that its concentration is higher than ≈0.02 ng g^{-1}.

Compared to ICP-MS, the proposed method has the advantage of an easier control of the spectral interferences and the use of a cheaper instrumentation. Of course, ICP-MS remains the analytical technique of choice whenever the study includes other trace elements, typically occurring below the ng g^{-1} concentration level. The method could also be considered as an

interesting alternative to ion chromatography, which is limited to the determination of Na^+, K^+, Ca^{2+} and Mg^{2+} ions.

Conflicts of interest

There are no conflicts to declare.

Acknowledgments

Appendix A. Supplementary data

Supplementary data to this article can be found online at doi:

Table 1. ICP-OES instrumental and operating parameters.

Parameter	Setting
RF Power	studied: 950-1350 W; optimal: 1350 W
Plasma gas flow rate	12 L min^{-1}
Auxiliary gas flow rate	0.5 L min^{-1}
Nebulizer	PFA-ST Micro-concentric
Spray chamber	single pass, heated at 150 °C
Nebulizer gas pressure	studied: 0.15-0.35 MPa; optimal: 0.15 MPa [*]
Sheathing gas flow rate	studied: 0.1-0.3 L min^{-1}; optimal: 0.1 L min^{-1}
Sample uptake rate	studied: 20-60 μL min^{-1}; optimal: 50 μL min^{-1}
Injector tube diameter	2.0 mm
Integration time	Low WL range: 15 s; High WL range: 5 s
Replicates	4
Wavelengths [#]	Al (*237.312*; 308.215; 309.271; 394.401; 396.152)
	Ba (230.424; 233.527; 455.403; *493.409*)
	Ca (315.887; 317.933; 393.366; 396.847; 422.673)
	Fe (238.204; 239.562; *240.488*; *259.837*; 259.940)
	K (766.490; 769.896)
	Mg (279.553; 280.270; 285.213; *383.230*; *383.829*)
	Na (589.592)
	Sr (*215.284*; 216.596; *346.446*; 407.771; 421.552)

Note: [*] corresponding to a flow rate of 0.5 L min^{-1} [#] values in nm. Lines in italic were considered for method development but not used for the analysis of samples.

Table 2. Instrumental performances.

Emission line (nm)	Range (ng mL^{-1})	Slope (cps ng^{-1}mL)	Improv. factor [*]	R^2	Instrumental precision [#]	Signal stability [§]
Al 237.312	0-500	0.72	2.4	0.998	0.8-2.9	3.3
Al 308.215	0-500	3.40	2.0	1.000	0.5-1.6	2.8
Al 309.271	0-500	5.96	1.9	1.000	0.3-0.8	2.6
Al 394.401	0-500	3.53	2.0	1.000	0.5-1.7	4.2
Al 396.152	0-500	14.8	1.8	1.000	0.3-1.7	3.7
Ba 230.424	0-10	17.5	2.0	1.000	0.7-2.1	3.6
Ba 233.527	0-10	19.8	2.1	1.000	0.8-2.1	2.5
Ba 455.403	0-10	834	2.0	1.000	0.3-1.4	2.9
Ba 493.409	0-10	438	2.1	1.000	0.4-1.9	2.6
Ca 315.887	0-1000	17.3	2.1	1.000	0.3-1.2	3.0
Ca 317.933	0-1000	22.5	1.7	1.000	0.4-1.1	3.3
Ca 393.366	0-1000	2330	1.9	1.000	0.5-1.2	2.8
Ca 396.847	0-1000	1390	1.9	1.000	0.4-1.4	3.1
Ca 422.673	0-1000	66.2	2.0	1.000	0.4-1.4	4.7
Fe 238.204	0-200	20.5	2.1	1.000	0.4-1.1	2.4
Fe 239.562	0-200	17.8	2.2	1.000	0.2-1.5	3.1
Fe 240.488	0-200	5.78	2.1	1.000	0.5-1.6	3.5
Fe 259.837	0-200	7.40	2.0	1.000	0.5-1.0	3.3
Fe 259.940	0-200	26.9	2.1	1.000	0.2-1.6	3.6
K 766.490	0-1000	31.1	1.3	0.999	0.4-1.2	5.1
K 769.896	0-1000	15.0	1.5	0.999	0.3-1.3	5.3
Mg 279.553	0-1000	837	2.1	1.000	0.4-2.0	2.1
Mg 280.270	0-1000	353	2.6	1.000	0.3-1.3	2.1
Mg 285.213	0-1000	52.3	2.0	1.000	0.3-1.0	2.8
Mg 383.230	0-1000	3.71	1.8	1.000	0.6-1.1	3.2
Mg 383.829	0-1000	6.78	2.1	1.000	0.3-1.5	4.2
Na 589.592	0-10000	94.7	1.7	1.000	0.6-2.0	4.6
Sr 215.284	0-10	5.99	2.1	1.000	1.3-5.3	3.3
Sr 216.596	0-10	9.27	2.2	1.000	0.7-3.0	3.1
Sr 346.446	0-10	14.2	1.7	0.996	3.9-8.5	2.4
Sr 407.771	0-10	1350	2.1	1.000	0.4-1.4	3.5
Sr 421.552	0-10	914	1.9	1.000	0.2-1.0	2.4

Notes: [*] compared to PFA / Cinnabar spray chamber (NP=0.27 MPa). [#] Min-max %RSD values of ten replicated analyses of Standard 3 (see Table S1 (Appendix)). [§] Signal variation for ten replicated analyses of Standard 3 during a 3-h analytical session.

Table 3. Recovery, precision, procedural blank and limits of detection of the analytical procedure

Emission line (nm)	Recovery (%) [*]		%RSD[#]	Blank[§] (ng g^{-1})	LOD[§] (ng g^{-1})
	Low conc	High conc			
Al 308.215	112±3	103±6	4.2	1.11	0.11
Al 309.271	103±2	100±7	4.8	1.39	0.41
Al 394.401	108±5	102±6	4.8	1.13	0.15
Al 396.152	109±3	102±6	4.3	1.13	0.10
Ba 230.424	81±5	97±2	3.7	0.011	0.015
Ba 233.527	82±2	95±2	2.2	0.011	0.013
Ba 455.403	83±2	94±1	1.9	0.011	0.013
Ca 315.887	101±3	101±4	3.6	0.76	0.52
Ca 317.933	100±3	101±4	3.3	0.74	0.52
Ca 393.366	99±2	102±2	2.3	0.76	0.53
Ca 396.847	99±3	96±3	3.0	0.75	0.54
Ca 422.673	99±3	102±4	3.7	0.76	0.52
Fe 238.204	103±6	100±3	4.7	0.08	0.13
Fe 239.562	102±6	99±4	4.6	0.09	0.13
Fe 259.940	102±6	99±4	4.6	0.08	0.13
K 766.490	92±1	107±1	1.1	0.11	0.38
K 769.896	92±1	108±1	1.2	0.09	0.41
Mg 279.553	101±1	95±1	1.0	0.21	0.04
Mg 280.270	101±1	95±1	1.2	0.21	0.04
Mg 285.213	101±1	97±1	1.3	0.21	0.04
Na 589.592	96±2	102±1	1.5	0.28	0.39
Sr 216.596	100±3	98±1	2.2	0.001	0.004
Sr 407.771	100±1	97±1	0.8	0.001	0.003
Sr 421.552	100±1	97±1	0.9	0.002	0.003

Notes: [*] evaluated by triplicate analysis of 100-fold diluted standard 2 (low concentration) and standard 3 (high concentration); [#] pooled standard deviation (n=6); [§] mean value and three times the standard deviation of ten procedural blanks.

Table 4. Analysis of the certified reference water NIST SRM 1640a [*]

Analyte	Certified [#] (ng g^{-1})	Found (ng g^{-1})
Al	2.63±0.09	2.81±0.08
Ba	0.0753±0.0004	0.069±0.002
Ca	2.785±0.008	2.87±0.07
Fe	1.83±0.09	1.71±0.03
K	28.8±0.1	28.2±0.5
Mg	52.5±0.2	52.7±1.3
Na	156±2	160±3
Sr	0.0625±0.0004	0.060±0.003

Notes: [*] The uncertainty associated to each value is the expanded uncertainty about the mean calculated according to the GUM guideline, at 95 % level of confidence. [#] After 20-fold dilution Al, Fe, K, Mg, Na and 2000-fold dilution for Ba, Ca and Sr.
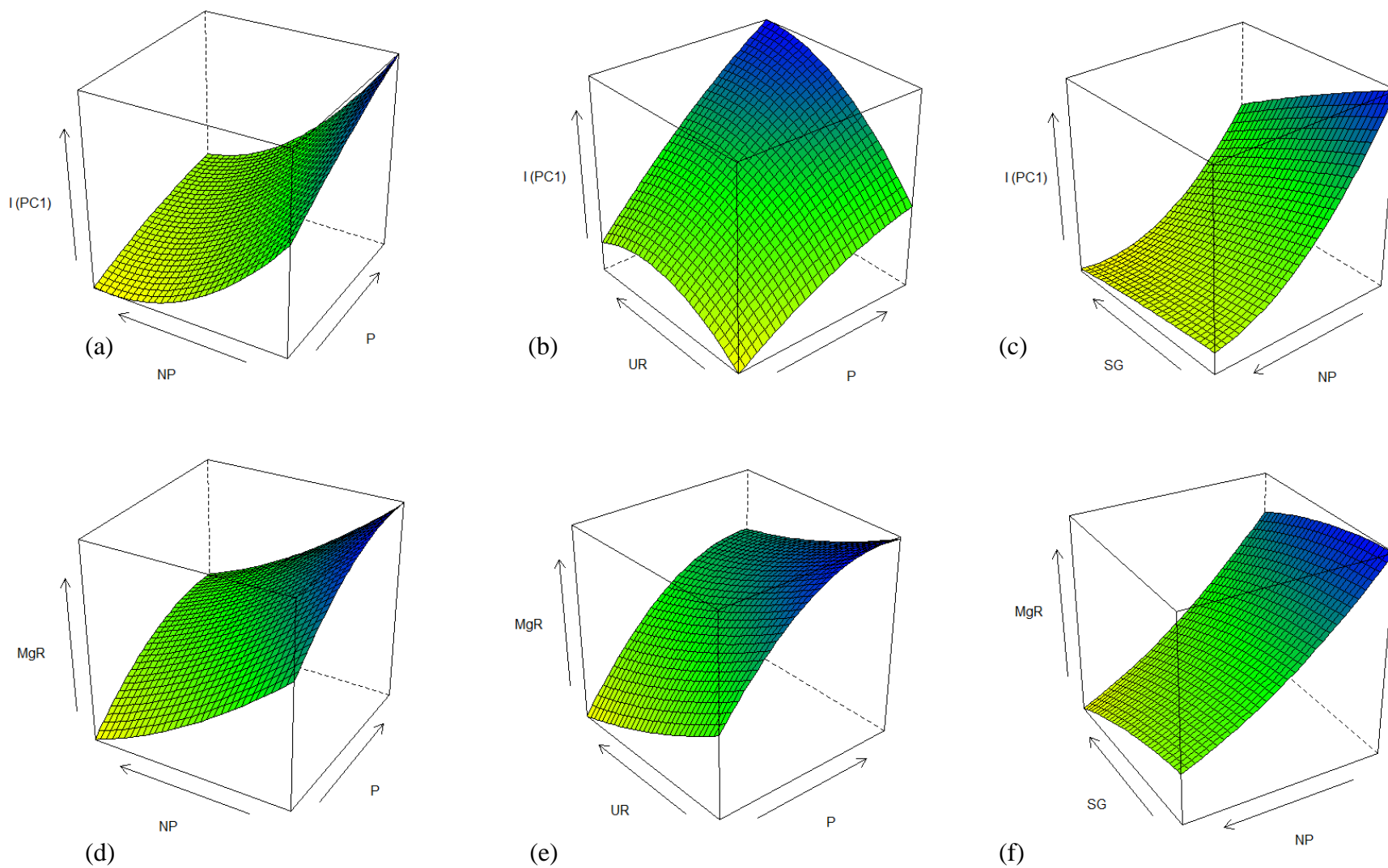
Figure 1. Combined effect of operating parameters on (a-c) sensitivity (score on PC1, see 3.1 for explanation) and (d-f) plasma robustness (Mg II 280.270 nm to Mg I 285.213 nm intensity ratio). P=RF power; NP=Nebulizer gas pressure; SG= Sheathing gas flow rate; UR=Sample uptake rate. In each graph, the two remaining variables are set at their center value.
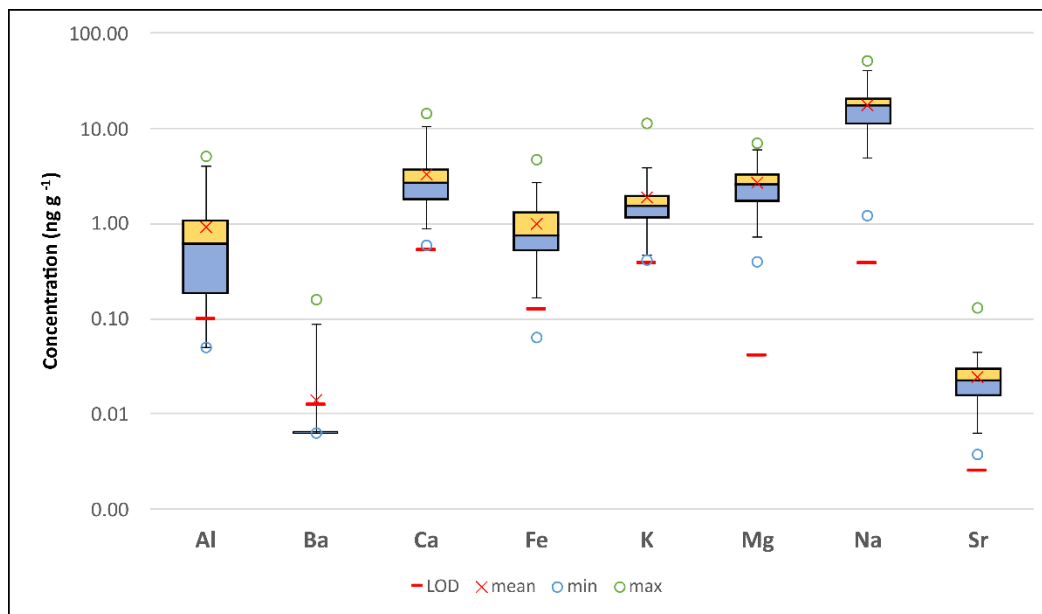
Figure 2. Major element concentrations in snow pit samples collected at Dome C. Boxes include data between 1st and 3rd quartile, divided by the median. Whiskers are 2.5th and 97.5th percentiles.

References

[1] J. R. Petit, J. Jouzel, D. Raynaud, N. I. Barkov, J.-M. Barnola, I. Basile, M. Bender, J. Chappellaz, M. Davis, G. Delaygue, M. Delmotte, V. M. Kotlyakov, M. Legrand, V. Y. Lipenkov, C. Lorius, L. PÉpin, C. Ritz, E. Saltzman and M. Stievenard, *Nature*, 1999, **399**, 429–436.

[2] EPICA community members, *Nature*, 2004, **429**, 623–628.

[3] M. Legrand, P. Mayewski, *Rev. Geophys.*, 1997, **35**, 219–243.

[4] N. Bertler, P. A. Mayewski, A. Aristarain, P. Barrett, S. Becagli, R. Bernardo, S. Bo, X. C, M. Curran, Q. D, D. Dixon, F. Ferrona, H. Fischer, M. Frey, M. Frezzotti, F. Fundel, C. Genthon, R. Gragnani, G. Hamilton, M. Handley, S. Hong, E. Isaksson, K. J, R. J, K. Kamiyama, S. Kanamori, E. Kärkäs, L. Karlöf, S. Kaspari, K. Kreutz, E. Meyerson, A. Kurbatov, Y. Ming, Z. M, H. Motoyama, R. Mulvaney, H. Oerter, E. Osterberg, M. Proposito, A. Pyne, U. Ruth, J. Simões, B. Smith, S. Sneed, K. Teinilä, F. Traufetter, R. Udisti, A. Virkkula, O. Watanabe, B. Williamson, J.-G. Winther, L. Y, E. Wolff, L. Z and A. Zielinski, *Ann. Glaciol.*, 2005, **41**, 167–179.

[5] S. Benassai, S. Becagli, R. Gragnani, O. Magand, M. Proposito, I. Fattori, R. Traversi, R., *Ann. Glaciol.*, 2005, 41, 32–40.

[6] B.R. Williamson, K.J. Kreutz, P.A. Mayewski, N.A.N. Bertler, S. Sneed, M. Handley, D. Introne, *J. Glaciol.*, 2007, **53**, 691–693.

[7] M. Ikegawa, M. Kimura, K. Honda, I. Akabane, K. Makita, H. Motoyama, F. Yoshiyuki, Y. Itokawa, *Atmos. Environ.,* 1999, **33**, 1457–1467.

[8] P. Vallelonga, P. Gabrielli, K. J. R. Rosman, C. Barbante, C. F. Boutron, *Geophys. Res. Lett.*, 2005, **32**, L01706.

[9] R. Röthlisberger, M. Bigler, E.W. Wolff, F. Joos, E. Monnin, M. A. Hutterli, *Geophys. Res. Lett.*, 2004, **31**, L16207.

[10] E. W. Wolff, H. Fischer, F. Fundel, U. Ruth, B. Twarloh, G. C. Littot, R. Mulvaney, R. Röthlisberger, M. de Angelis, C. F. Boutron, M. Hansson, U. Jonsell, M. A. Hutterli, F. Lambert, P. Kaufmann, B. Stauffer, T. F. Stocker, J. P. Steffensen, M. Bigler, M. L. Siggaard-Andersen, R. Udisti, S. Becagli, E. Castellano, M. Severi, D. Wagenbach, C. Barbante, P. Gabrielli and V. Gaspari, *Nature*, 2006, **440**, 491–496.

[11] K. Liu, S. Hou, S. Wu, H. Pang, W. Zhang, J. Song, J. Yu, X. Zou, J. Wang, *Atmos. Res.*, 2021, **248**, 105263.

[12] C.F. Buck, P.A. Mayewski, M.J. Spencer, S. Whitlow, M.S. Twickler, D. Barrett, *J. Chromatogr. A*, 1992, **594**, 225–228.

[13] K.A. Welch, W.B. Lyons, E. graham, K. Neumann, J.M. Thomas, D. Mikesell, *J. Chromatogr. A*, 1996, **739**, 257–263.

[14] G.C. Littot, R. Mulvaney, R. Röthlisberger, R. Udisti, E.W. Wolff, E. Castellano, M. De Angelis, M.E. Hansson, S. Sommer, J.P Steffensen, *Ann. Glaciol.*, 2002, **35**, 299–305.

[15] N.A.N. Bertler, P.A. Mayewski, P.J. Barrett, S.B. Sneed, M.J. Handley, K.J. Kreutz, *Ann. Glaciol.*, 2004, **39**, 139–145.

[16] M. Grotti, F. Soggia, F. Ardini, E. Magi, *J. Environ. Monit.*, 2011, **13**, 2511–2520.

[17] M. Grotti, F. Soggia, F. Ardini, E. Magi, S. Becagli, R.Traversi , R. Udisti, *Chemosphere*, 2015, **138**, 916–923.

[18] D.A. Dixon, P.A. Mayewski, E. Korotkikh, S.B. Sneed, M.J. Handley, D.S. Introne, T.A. Scambos, *The Cryosphere*, 2013, **7**, 515–535.

[19] K.A. Casey, S.D. Kaspari, S.M. Skiles, K. Kreutz, M.J. Handley, *J. Geophys. Res. Atmos.*, 2017, **122**, 6592–6610.

[20] E. Paredes, M. Grotti, J. M. Mermet and J. L. Todoli, *J. Anal. At. Spectrom.*, 2009, **24**, 903–910.

[21] M. Grotti, F. Ardini and J. L. Todoli, *Anal. Chim. Acta*, 2013, **767**, 14–20.

[22] F. Ardini, M. Grotti, R. Sanchez and J. L. Todoli, *J. Anal. At. Spectrom.*, 2012, **27**, 1400–1404.

[23] S. Bertinetti, F. Ardini, M.A. Vecchio, L. Caiazzo, M. Grotti, *Chemosphere* 2020, 255, 126858.

[24] M. Grotti, F. Soggia, J.L. Todolì, *Analyst*, 2008, **133**, 1388–1394.

[25] F. Ardini, A. Bazzano, M. Grotti, *J. Anal. At. Spectrom.*, 2018, **33**, 2124–2132.

[26] G.E.P. Box, W.G. Hunter and J.S. Hunter, *Statistics for experimenters*, Wiley, New York, 1978.

[27] R Core Team (2020). R: A language and environment for statistical computing. R Foundation for Statistical Computing, Vienna, Austria. URL: https://www.R-project.org (last access XXth May 2021).

[28] R. Leardi, C. Melzi and G. Polotti, CAT (Chemometric Agile Tool), freely downloadable from http://gruppochemiometria.it/index.php/software (last access XXth May 2021).

[29] J.M. Mermet, *Anal. Chim. Acta*, 1991, **250**, 85–94.

[30] A. Bazzano, K. Latruwe, M. Grotti, F. Vanhaecke, *J. Anal. At. Spectrom.*, 2015, **30**, 1322–1328.

[31] BIPM, IEC, IFCC, ISO, IUPAC, IUPAP and OIML, Guide to expression of uncertainty in measurement, 2nd edn, 1995, ISBN 92-67-10188-9.